Acta Cryst. (1999). B**55**, 867–881

The use of CCD area detectors in charge-density research. Application to a mineral compound: the α-spodumene $LiAl(SiO_3)_2$

Sandrine Kuntzinger,[a] Slimane Dahaoui,[b] Nour Eddine Ghermani,[a]* Claude Lecomte[a] and Judith A. K. Howard[b]

[a]*Laboratoire de Cristallographie et Modélisation des Matériaux Minéraux et Biologiques, LCM3B, UPRES A CNRS 7036, Université Henri Poincaré, Nancy 1, Faculté des Sciences, Boulevard des Aiguillettes, BP 239, 54506 Vandoeuvre-lès-Nancy CEDEX, France, and* [b]*Crystallography Group, Department of Chemistry, University of Durham, South Road, Durham DH1 3LE, England. E-mail: ghermani@lcm3b.u-nancy.fr*

(*Received 15 February 1999; accepted 19 May 1999*)

Abstract

X-ray diffraction data sets collected on both Nonius and Siemens (Bruker) goniometers equipped with charge-coupled device (CCD) area detectors have been tested for the electron-density determination of the aluminosilicate mineral compound α-spodumene $LiAl(SiO_3)_2$, aluminium lithium silicon oxide. Data collection strategies, reflection intensity peak integration methods and experimental error estimates are different for the two instruments. Therefore, the consistency and quality of the two types of CCD measurements have been carefully compared to each other and to high-resolution data collected on a conventional CAD-4 point-detector diffractometer. Multipole density model refinements were carried out against the CCD data and the statistical factors analysed in terms of experimental weighting schemes based on the standard uncertainties of the diffraction intensities derived by the Nonius and Siemens software programs. Consistent experimental electron-density features in the Si–O–Si and Si–O–Al bridges were found from both CCD data sets. The net atomic charges obtained from the kappa refinements against each CCD data set are also in good agreement and quite comparable with the results of the conventional CAD-4 experiment.

1. Introduction

High-resolution X-ray diffraction is nowadays the main experimental approach to obtain the electron density distribution in crystals. The diffraction data filtered by multipole pseudo-atom models yield an accurate insight into the chemical bonding and the atomic interactions in different kinds of solid-state materials. High-quality data are necessary for charge-density studies and to date the laboratory four-circle diffractometer (CAD-4) equipped with a scintillation counter has largely proved satisfactory for this purpose. However, the main constraint in such experiments is the data collection time, which can even reach several months (Pichon-Pesme *et al.*, 1994) for crystals with large unit cells, since each reflection intensity is measured sequentially. In addition, the diffraction experiment becomes more difficult when low temperature or any other crystal physical constraint is used, and the experiment is often impossible for chemically or time-degradable samples. Initially used in protein crystallography, area detectors, such as imaging plates, are able to record many diffraction intensities at a time. This capability overcomes some of the problems and disadvantages of conventional point-detector CAD-4 experiments. In the charge-density field, the use of area detectors with synchrotron X-ray radiation has been successfully demonstrated by Bolotovsky *et al.* (1995) (see also Coppens *et al.*, 1997). In the past decade, the technological application of the CCD chip to X-ray radiation detection has permitted construction of more sensitive and practical area counters (Allinson, 1994) than the imaging plates. Early work on the performance and advantages of CCD detectors was related to synchrotron radiation experiments (see for example Graafsma, Svensson & Kvick, 1997; Koritsanszky *et al.*, 1998; Graafsma, Souhassou *et al.*, 1997, 1998). CCD area detectors are now also adapted to conventional laboratory radiation sources, and in recent years many studies of their use in accurate high-resolution X-ray diffraction experiments have been reported. Careful inspections of data quality and comparisons with CAD-4 intensities have been carried out (see for example Pinkerton, 1997; Martin & Pinkerton, 1998; Macchi, Proserpio & Sironi, 1998; Macchi, Proserpio, Sironi, Soave & Destro, 1998; Dahaoui *et al.*, 1999) in order to test this new detector in the field of experimental charge-density research. However, all these studies dealt with organic or organometallic materials and only one CCD diffractometer [the Siemens (Bruker) instrument] was available for testing. In this paper, we report a study of the electron density in a natural aluminosilicate mineral compound, the α-spodumene $LiAl(SiO_3)_2$ (monoclinic phase, space group $C2/c$), from X-ray diffraction CCD data sets collected at room temperature on both the Siemens (Smart CCD) and the recently developed Nonius (Kappa CCD) platform. Our analysis

involves numerous experimental variables: two different samples were used; two X-ray radiations, Mo $K\alpha$ for Siemens and Ag $K\alpha$ for Nonius; use of data collection strategies and processing inherent to each system; different measurement redundancies and different rates of data acquisition. In addition, statistical aspects related to the experimental weighting schemes used in the refinements are discussed. A comparison is also made with the results of a conventional CAD-4 electron-density study, employing both Mo $K\alpha$ and Ag $K\alpha$ radiation, reported recently by Kuntzinger & Ghermani (1999).

2. Experimental

2.1. *Nonius Kappa CCD data collection*

The same natural spodumene parallelepipedic crystal (of dimensions 0.36 × 0.18 × 0.06 mm) as that used in the previous CAD-4 electron-density study (Kuntzinger & Ghermani, 1999) was mounted on the four-circle Nonius Kappa CCD diffractometer equipped with a CCD area detector at the Nonius company test laboratory in Delft (The Netherlands). The experiment was carried out at room temperature using graphite-monochromated Ag $K\alpha$ (λ = 0.56087 Å) X-ray radiation. Two crystal-to-detector distances were chosen for the data collection: 30 mm (data set I) up to a maximum reciprocal resolution of $(\sin\theta/\lambda)_{max}$ = 1.43 Å^{-1} and 50 mm (data set II) up to $(\sin\theta/\lambda)_{max}$ = 1.0 Å^{-1}. The latter crystal-to-detector distance was chosen in order to try to improve the statistics of the low-resolution intensities strongly affected by the atomic valence density. The *COLLECT* program of the Nonius Kappa CCD software package (Nonius, 1998) was used in order to determine and optimize the goniometer and detector angular positions during the data collection. The frames were recorded using $\Delta\omega$ = 1° rotation scans, corresponding to a rotation of $\Delta\varphi$ = 1° when the κ and ω goniometer angles are at the 0 and 180° positions, respectively. The choice of rotation angles was restricted by the limited number of frames (1000) which can be treated by the image-scaling program *SCALEPACK* of the Nonius Kappa CCD software package (Nonius, 1998). For this reason, only half of the Ewald sphere was measured for α-spodumene. Set I data were collected with an acquisition time of 100 s per frame in order to ensure the measurement of the high-resolution weak intensities. The low-to-medium resolution set II reflections were recorded with an exposure time of 25 s per frame in order to avoid CCD detector saturation by strong intensities. 972 frames were measured during 55 h for data set I, compared with 430 h for Ag $K\alpha$ CAD-4 data collection (Kuntzinger & Ghermani, 1999). The data set II acquisition of 1049 frames took 15 h. Each image was recorded twice in order to eliminate the so-called 'zinger' spots originating from cosmic radiation and detected by the CCD counter. Reflection indexing, Lorentz–polarization correction, peak integration and background determination were performed using the program *DENZO* of the Kappa CCD software package (Nonius, 1998). With the *DENZO* program, the intensity and background are integrated inside boxes and the peak profile limits are defined inside circular or elliptical spot shapes (useful only when the goniometer angle κ is set to 0°). The box and spot dimensions are given by the user relative to the intensity spot area. The user's guide recommends a box to spot area ratio of 2. The estimation of the integrated intensity in each frame is performed following the profile fitting procedure (Diamond, 1969). In the case of α-spodumene, the low-resolution strong intensities present large and intense spots in comparison to those belonging to the medium- or high-resolution region. In the frame collection of data set I, the box size of 35 × 35 pixels (each pixel has a dimension of *ca* 80 µm for the Nonius CCD detector) was used for the integration of all observed intensities. For data set II, two box sizes were used: 35 × 35 pixels for low-resolution and 38 × 38 pixels for high-resolution intensities to take into account spot broadening for high Bragg angles. The available software version did not take into account the $K\alpha_1$–$K\alpha_2$ radiation splitting occurring at higher resolution. Finally, the frame-to-frame intensity scaling and experimental error estimates were derived using the *SCALEPACK* program included in the Nonius software package. This program also takes into account the partial spots on the successive images in order to retrieve the full reflection intensity.

The unit-cell parameters and the orientation matrix were initially determined from the first ten measured frames of the data, and then refined during the indexing and the intensity integration process using *DENZO* with all the recorded images. Afterwards, in the case of several data sets, the *SCALEPACK* program averages the unit-cell parameters obtained with each data set. The results of our experiment are a = 9.479 (1), b = 8.407 (1), c = 5.226 (1) Å and β = 110.17 (1)° from data set I and a = 9.475 (1), b = 8.403 (1), c = 5.225 (1) Å and β = 110.16 (1)° from data set II; the CAD-4 Ag $K\alpha$ values (Kuntzinger & Ghermani, 1999) are a = 9.456 (1), b = 8.386 (1), c = 5.216 (1) Å and β = 110.13 (1)°, based on the angular settings of 25 reflections (see Table 1). Also for comparison, the lattice parameters obtained from a powder diffraction experiment by Clark *et al.* (1969) are a = 9.449 (3), b = 8.386 (1), c = 5.215 (2) Å and β = 110.10 (2)°.

An empirical absorption correction was applied with the modified *SORTAV* (Blessing, 1995) program in the Nonius Kappa CCD software package (Nonius, 1998). The transmission factors are given in Table 1 and compared to those of the other experiments. The internal agreement factors after the data merging and averaging in Laue group 2/*m* and supplementary

Table 1. *Details of the experimental diffraction data collections*

The agreement indices are defined as follows:

$$R_1 = \sum_H \sum_i^{N(H)} |Y_i - \bar{Y}| \Big/ \sum_H \sum_i^{N(H)} |Y_i|,$$
$$R_2 = \Big[\sum_H \sum_i^{N(H)} (Y_i - \bar{Y})^2 \Big/ \sum_H \sum_i^{N(H)} (Y_i)^2 \Big]^{1/2},$$
$$wR = \Big\{ \Big[\sum_H \sum_i^{N(H)} (Y_i - \bar{Y})^2 / \sigma^2(Y) \Big] \Big/ \Big[\sum_H \sum_i^{N(H)} (Y_i)^2 / \sigma^2(Y) \Big] \Big\}^{1/2},$$
$$Z = \Big(\Big[N_{\text{terms}} / (N_{\text{terms}} - N_{\text{means}}) \Big] \Big\{ \Big[\sum_H \sum_i^{N(H)} (Y_i - \bar{Y})^2 / \sigma^4(Y) \Big] \Big/ \Big[\sum_H \sum_i^{N(H)} 1/\sigma^2(Y) \Big] \Big\} \Big)^{1/2},$$

where $Y = |F_o|^2$ (arbitrary scale) is the square of the observed structure factor, $\sigma^2(Y) = 1/w$ is the experimental variance, w is the statistical weight, $N(H)$ is the number of equivalents (or redundants) for each reflection, and N_{terms} and N_{means} are the total number of the reflections and the number of the unique reflections, respectively.

			Nonius Kappa CCD		
	Nonius CAD-4	Nonius CAD-4	Set I	Set II	Siemens Smart CCD
Generator electric inputs: voltage (kV)/current (mA)	–	–	50/40	50/40	50/40
Radiation type, wavelength (Å)	Ag $K\alpha$, 0.56087	Mo $K\alpha$, 0.71073	Ag $K\alpha$, 0.56087	Ag $K\alpha$, 0.56087	Mo $K\alpha$, 0.71073
a (Å)	9.456 (1)	9.462 (1)	9.479 (1)	9.475 (1)	9.4846 (5)
b (Å)	8.386 (1)	8.392 (1)	8.407 (1)	8.403 (1)	8.4121 (4)
c (Å)	5.216 (1)	5.221 (1)	5.226 (1)	5.225 (1)	5.2308 (4)
β (°)	110.13 (1)	110.18 (1)	110.17 (1)	110.16 (1)	110.17 (2)
V (Å^3)	388.36 (9)	389.12 (8)	390.93 (3)	390.52 (3)	391.75 (3)
$(\sin\theta/\lambda)_{\max}$ (Å^{-1})	1.26	1.22	1.43	1.00	1.09
Scan method	ω–2θ scan	ω–2θ scan	1° $\Delta\omega$ scan	1° $\Delta\omega$ scan	0.2° $\Delta\omega$ scan
Crystal to detector distance (d, mm)	–	–	30	50	45
Total No. of frames per exposure/time per frame (t) (s)	–	–	972/100	1049/25	13 566/10
Total exposure time (h)	430	298	55	15	50
Absorption correction $T_{\min}/T_{\max}$	0.82/0.97	0.68/0.95	0.89/0.95	0.89/0.94	0.76/0.98
Total No. of measurements	15 850	12 984	22 419	9639	23 705
Total No. of reflections	15 849	12 933	21 629	9537	23 591
Unique intensities (including negative)/lattice	3241/3254	2945/2960	4529/4788	1620/1636	2112/2125
No. of observed reflections [$I > 3\sigma(I)$]	2261	2366	3692	1362	1743
R_1	0.021	0.021	0.033	0.024	0.026
R_2	0.028	0.033	0.044	0.033	0.034
wR	0.025	0.021	0.041	0.030	0.016
Z	0.88	0.90	0.90	0.85	1.14

experimental details for the two Nonius data set collections are summarized in Table 1.

2.2. *Siemens Smart CCD data collection*

Another, slightly larger parallelepiped sample (0.44 × 0.16 × 0.08 mm) was cut from the same large original spodumene block used to extract the crystal for the CAD-4 and Nonius Kappa CCD experiments. The X-ray diffraction measurements on a Siemens Smart CCD diffractometer were also carried out at room temperature, but using graphite-monochromated Mo $K\alpha$ (λ = 0.71073 Å) radiation. In this experiment, the crystal was positioned at a distance of 45 mm from the CCD area-detector entry. The *ASTRO* program of the Smart CCD software package (Siemens, 1996) was used to collect a full Ewald sphere of data up to a reciprocal resolution of $(\sin\theta/\lambda)_{\max} = 1.09$ Å^{-1}. Each frame was recorded as an ω scan of 0.2° in order to reconstruct accurate three-dimensional reflection profiles with an X-ray exposure time equal to 10 s. 13 566 frames were collected in this experiment during a crystal irradiation time of 50 h; some frames are recorded twice because of the detector saturation for strong reflections. With the Siemens software (*SAINT*; Siemens, 1996), a global box size and the intensity peak width are defined in degrees related to the sample-to-detector distance and to the broadening of the spots. In our experiment, these parameters were chosen as follows: X and Y box dimensions equal to 1.2° and a half-peak width of 0.6° for low-resolution data. These parameters were multiplied by a factor of 1.5 for high-resolution intensities in order to take into

Table 2. *Agreement merging and averaging indices (defined in Table 1) with respect to* $s = \sin\theta/\lambda$ *(Å*$^{-1}$*) and* $Y = |F_o|^2$ *(arbitrary scale) ranges for the three CCD data sets*

s interval	R_1	R_2	wR	Z	Number of terms	Number of means	Unique measured
Nonius Kappa CCD set I							
$s < 0.500$	0.0312	0.0474	0.0250	0.934	2042	203	203
$0.500 < s < 0.600$	0.0281	0.0371	0.0285	0.927	1425	147	147
$0.600 < s < 0.650$	0.0275	0.0360	0.0273	0.901	872	94	94
$0.650 < s < 0.700$	0.0289	0.0360	0.0298	0.897	1002	112	112
$0.700 < s < 0.750$	0.0272	0.0336	0.0298	0.817	1112	133	133
$0.750 < s < 0.800$	0.0310	0.0385	0.0354	0.940	1232	154	154
$0.800 < s < 0.850$	0.0311	0.0415	0.0356	0.897	1201	160	160
$0.850 < s < 0.900$	0.0338	0.0403	0.0394	0.804	1371	192	192
$0.900 < s < 0.950$	0.0386	0.0452	0.0449	0.879	1422	209	211
$0.950 < s < 1.000$	0.0396	0.0403	0.0517	0.879	1392	231	234
$1.000 < s < 1.050$	0.0439	0.0478	0.0569	0.933	1480	252	255
$1.050 < s < 1.100$	0.0554	0.0588	0.0693	0.861	1565	278	287
$1.100 < s < 1.150$	0.0606	0.0597	0.0758	0.850	1377	283	304
$1.150 < s < 1.200$	0.0711	0.0644	0.0959	0.899	1359	302	340
$1.200 < s < 1.250$	0.0933	0.0995	0.1025	0.768	1274	298	359
$1.250 < s < 1.300$	0.0675	0.0728	0.0977	0.968	547	246	386
$1.300 < s < 1.350$	0.0859	0.0805	0.1228	1.038	468	214	395
$1.350 < s < 1.400$	0.0999	0.0915	0.1419	1.010	438	205	413
$1.400 < s < 1.450$	0.0831	0.0909	0.1227	0.921	50	25	149
Nonius Kappa CCD set II							
$s < 0.500$	0.0198	0.0349	0.0200	0.896	1808	207	207
$0.500 < s < 0.600$	0.0191	0.0221	0.0245	0.819	1273	147	147
$0.600 < s < 0.650$	0.0228	0.0282	0.0271	0.906	725	93	93
$0.650 < s < 0.700$	0.0253	0.0279	0.0308	0.845	828	112	112
$0.700 < s < 0.750$	0.0321	0.0335	0.0363	0.769	914	133	134
$0.750 < s < 0.800$	0.0336	0.0342	0.0414	0.804	955	149	149
$0.800 < s < 0.850$	0.0370	0.0364	0.0444	0.729	921	160	163
$0.850 < s < 0.900$	0.0491	0.0482	0.0568	0.691	892	181	192
$0.900 < s < 0.950$	0.0669	0.0643	0.0755	0.814	859	196	210
$0.950 < s < 1.000$	0.0514	0.0469	0.0639	0.784	362	141	213
Siemens Smart CCD							
$s < 0.500$	0.0260	0.0367	0.0146	2.463	4260	192	207
$0.500 < s < 0.600$	0.0238	0.0286	0.0129	0.791	3732	146	149
$0.600 < s < 0.650$	0.0240	0.0299	0.0142	0.733	2349	92	93
$0.650 < s < 0.700$	0.0234	0.0273	0.0123	0.745	2252	111	112
$0.700 < s < 0.750$	0.0248	0.0285	0.0210	0.670	1364	134	134
$0.750 < s < 0.800$	0.0239	0.0264	0.0208	0.697	1382	149	152
$0.800 < s < 0.850$	0.0251	0.0273	0.0220	0.657	1424	158	159
$0.850 < s < 0.900$	0.0300	0.0307	0.0265	0.700	1621	193	194
$0.900 < s < 0.950$	0.0324	0.0318	0.0291	0.684	1673	207	207
$0.950 < s < 1.000$	0.0318	0.0305	0.0292	0.697	1645	225	232
$1.000 < s < 1.050$	0.0355	0.0358	0.0320	0.747	1481	234	251
$1.050 < s < 1.100$	0.0387	0.0390	0.0431	0.787	408	157	222

Y interval	R_1	R_2	wR	Z	Number of terms	Number of means
Nonius Kappa CCD set I						
$0.0 < Y < 1.0$	0.9909	0.9837	0.9813	0.663	100	22
$1.0 < Y < 3.0$	0.8776	0.9149	0.7950	0.682	348	64
$3.0 < Y < 10.0$	0.5754	0.6388	0.4216	0.902	1108	239
$10.0 < Y < 30.0$	0.2543	0.3234	0.1867	0.867	1793	364
$30.0 < Y < 100.0$	0.1192	0.1612	0.0878	1.007	2860	583
$100.0 < Y < 300.0$	0.0793	0.1078	0.0611	1.050	3777	718
$300.0 < Y < 1000.0$	0.0480	0.0644	0.0383	0.879	4685	806
$1000.0 < Y < 3000.0$	0.0320	0.0421	0.0280	0.741	3577	513
$3000.0 < Y < 10000.0$	0.0276	0.0374	0.0237	0.687	2290	267
$10000.0 < Y < 30000.0$	0.0306	0.0421	0.0243	0.729	768	82
$30000.0 < Y < 100000.0$	0.0361	0.0529	0.0305	0.932	52	9
Nonius Kappa CCD set II						
$0.0 < Y < 1.0$	0.9651	0.9728	0.9401	0.524	170	30
$1.0 < Y < 3.0$	0.7386	0.8145	0.5782	0.656	279	49

Table 2 (*cont.*)

Y interval	R_1	R_2	wR	Z	Number of terms	Number of means
$3.0 < Y < 10.0$	0.3909	0.5115	0.2653	0.787	584	110
$10.0 < Y < 30.0$	0.1703	0.2191	0.1238	0.832	1054	171
$30.0 < Y < 100.0$	0.0858	0.1137	0.0631	1.035	1472	254
$100.0 < Y < 300.0$	0.0514	0.0692	0.0383	1.001	2032	337
$300.0 < Y < 1000.0$	0.0294	0.0387	0.0235	0.813	1974	299
$1000.0 < Y < 3000.0$	0.0188	0.0242	0.0175	0.674	1328	181
$3000.0 < Y < 10000.0$	0.0172	0.0236	0.0154	0.660	516	66
$10000.0 < Y < 30000.0$	0.0286	0.0445	0.0197	0.901	62	8
Siemens Smart CCD						
$0.0 < Y < 1.0$	0.8702	0.8981	0.8532	0.624	666	65
$1.0 < Y < 3.0$	0.5534	0.6069	0.4914	0.625	1006	102
$3.0 < Y < 10.0$	0.2026	0.2499	0.1815	0.616	2076	197
$10.0 < Y < 30.0$	0.0793	0.0998	0.0721	0.629	2981	289
$30.0 < Y < 100.0$	0.0402	0.0501	0.0357	0.723	4597	421
$100.0 < Y < 300.0$	0.0276	0.0349	0.0224	0.960	4518	419
$300.0 < Y < 1000.0$	0.0227	0.0288	0.0125	4.344	4814	332
$1000.0 < Y < 3000.0$	0.0227	0.0295	0.0114	2.718	2397	123
$3000.0 < Y < 10000.0$	0.0286	0.0386	0.0149	2.539	379	22

account the $K\alpha_1$–$K\alpha_2$ radiation splitting. Lorentz and polarization correction, data reduction and processing were also carried out using *SAINT* of the Smart CCD software package.

The unit-cell parameters were refined over a set of 512 reflections respecting the threshold intensity $I/\sigma(I) > 30$ in the resolution range 0.5–0.8 Å^{-1}: the results a = 9.4846 (5), b = 8.4121 (4), c = 5.2308 (4) Å and β = 110.17 (2)° are slightly larger than the CAD-4 Mo $K\alpha$ (Kuntzinger & Ghermani, 1999) values a = 9.462 (1), b = 8.392 (1), c = 5.221 (1) Å and β = 110.18 (1)° (Table 1), but the Siemens CCD results agree with those obtained from the Nonius Kappa CCD experiment.

Finally, the *SADABS* (Sheldrick, 1996; Siemens, 1996) program was used to apply an empirical absorption correction to the measurements (see Table 1 for transmission factors). We also note that no problem with $\lambda/2$ contamination was encountered in this data set, in contrast to a case previously described (Kirschbaum *et al.*, 1997). Data merging and averaging were also performed in Laue group 2/*m*; the internal agreement indices are given in Table 1.

3. Data analysis

3.1. *CCD data quality and comparison to CAD-4 measurements*

The manufacturers recommendations for the optimization of peak integration procedures (mainly the box and spot sizes for low- and high-resolution reflections) and for the estimation of the experimental error implemented in the Nonius and Siemens software packages (*DENZO* and *SCALEPACK* for Nonius, and *SAINT* for Siemens) impose system-specific data collection strategies, particularly for ω-scan rotation angles ($\Delta\omega$ = 1° for Nonius and 0.2° for Siemens). Furthermore, as given above, the frame acquisition time (t) and the crystal-to-detector distance (d) have been chosen differently, especially between Nonius data set I and set II experiments (see Table 1), in order to cover a part or all of a given reciprocal-space region. Nevertheless, the total CCD data collection time of 50 h still remains very short in comparison to that of CAD-4 scintillation-detector diffractometer data acquisition (430 h for Ag $K\alpha$ radiation and 298 h for Mo $K\alpha$ radiation; see Table 1).

In order to compare the quality of the respective data we present in Table 2 the merging agreement factors with respect to the $\sin\theta/\lambda$ ranges and as a function of the squared structure factors $|F_o|^2$ on the experimental arbitrary scale listed in the *SORTAV* program printout (Blessing, 1987, 1989). The Siemens Smart CCD data set displays more than double redundancy in the measurements compared to both the Nonius Kappa CCD data sets for low-resolution reflection intensities. This is firstly a result of our choice of full Ewald sphere scans in the case of Smart CCD data collection, but only half a sphere in the Kappa CCD measurements. Among the three CCD data sets and with respect to the reciprocal resolution, the Nonius Kappa CCD set II has the lowest agreement indices, especially for the range $0 < \sin\theta/\lambda < 0.6$ Å^{-1}. However, the differences in agreement factors involving the experimental weights, wR and Z factors (defined in Table 1), show that the standard errors are not similarly estimated by the two software packages. On the other hand, it is worth noting the missing unique reflections in the low-resolution region for the Kappa CCD data set I experiment: For $0 < \sin\theta/\lambda < 0.5$ Å^{-1} we have only 203 unique reflections, compared to 207 for Nonius set II and Siemens data. Four low-resolution reflections ($\bar{2}21$, 310, 020 and 002) overflowed the CCD detector pixels (with t = 100 s) and were rejected during the processing of Nonius data set I. On the contrary, for

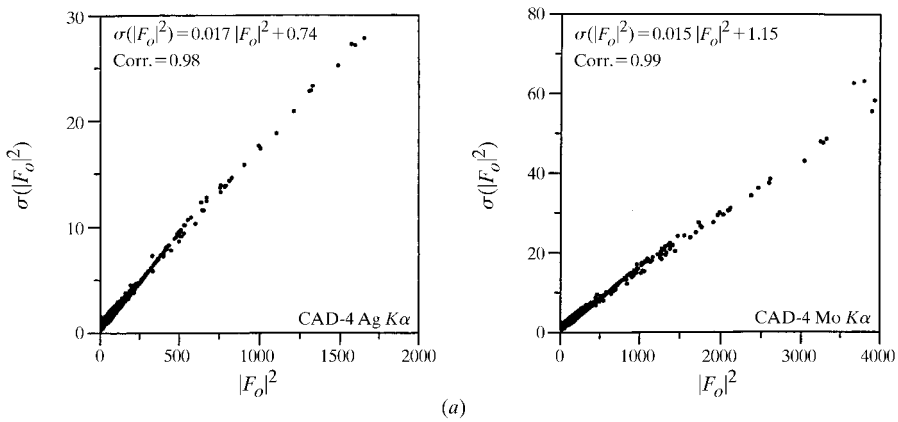

(*a*)

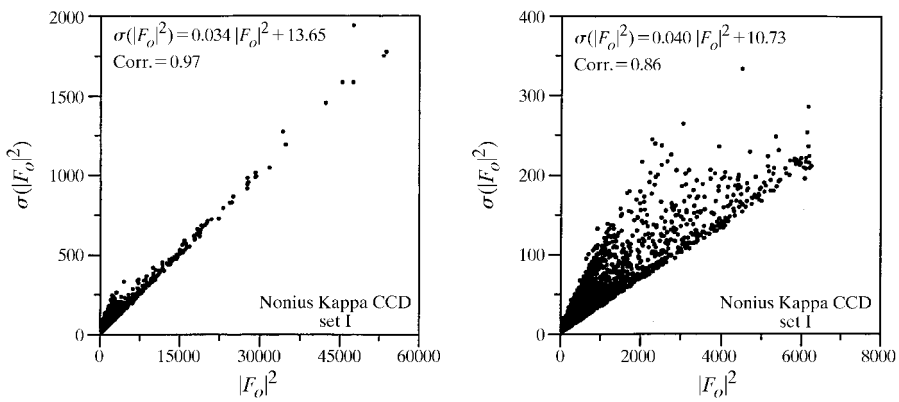

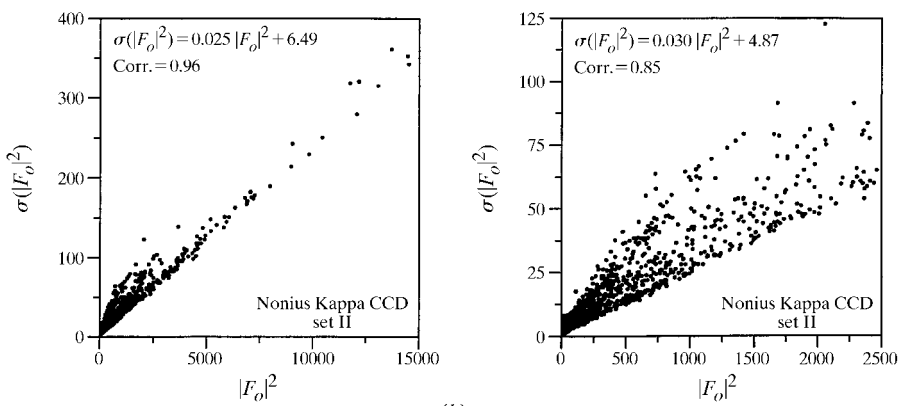

(*b*)

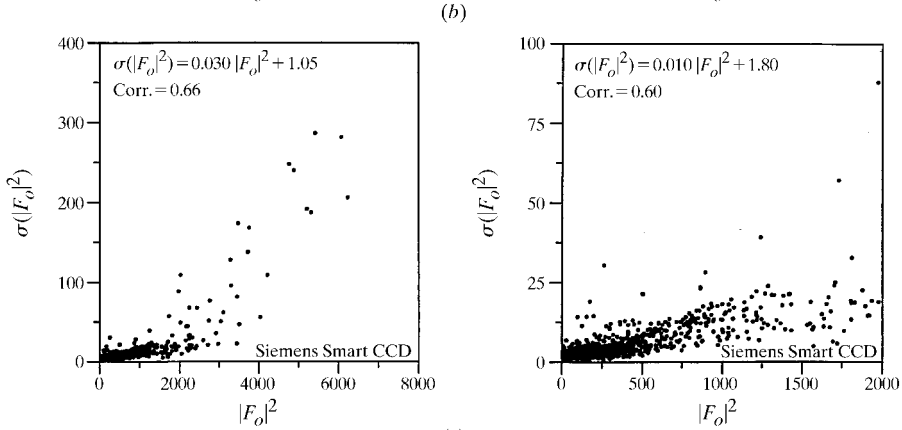

(*c*)

Fig. 1. Experimental errors *versus* the squared structure factors (in experimental arbitrary scale). (*a*) CAD-4 Ag $K\alpha$ and Mo $K\alpha$ radiation data. (*b*) Nonius Kappa CCD data set I and data set II. (*c*) Siemens Smart CCD measurements. (The linear regression fit and the correlation factors are indicated on each figure.) For (*b*) and (*c*) the plots on the right correspond to low-intensity data.

Table 3. *Agreement merging and averaging indices (defined in Table 1) with respect to* $s = \sin\theta/\lambda$ ($\mathring{A}^{-1}$) *and* $Y = |F_o|^2$ *(arbitrary scale) ranges for Ag Kα and Mo Kα radiation CAD-4 data sets*

CAD-4 data according to Kuntzinger & Ghermani (1999).

s interval	R_1	R_2	wR	Z	Number of terms	Number of means	Unique measured
Nonius CAD-4 Ag $K\alpha$ radiation							
$s < 0.500$	0.0181	0.0280	0.0143	0.789	3517	207	207
$0.500 < s < 0.600$	0.0155	0.0249	0.0162	0.821	908	145	145
$0.600 < s < 0.650$	0.0193	0.0253	0.0225	0.943	456	95	95
$0.650 < s < 0.700$	0.0183	0.0215	0.0208	0.862	430	110	110
$0.700 < s < 0.750$	0.0259	0.0269	0.0264	0.896	510	130	130
$0.750 < s < 0.800$	0.0288	0.0297	0.0291	0.845	587	151	151
$0.800 < s < 0.850$	0.0338	0.0313	0.0337	0.928	632	161	161
$0.850 < s < 0.900$	0.0422	0.0442	0.0361	0.868	737	188	188
$0.900 < s < 0.950$	0.0514	0.0465	0.0425	0.866	830	210	210
$0.950 < s < 1.000$	0.0558	0.0514	0.0450	0.907	923	238	238
$1.000 < s < 1.050$	0.0556	0.0467	0.0462	0.964	998	252	252
$1.050 < s < 1.100$	0.0732	0.0595	0.0555	0.970	1115	284	284
$1.100 < s < 1.150$	0.0947	0.0752	0.0656	0.895	1200	303	304
$1.150 < s < 1.200$	0.1092	0.0826	0.0732	0.928	1312	335	335
$1.200 < s < 1.250$	0.1366	0.1161	0.0861	0.928	1452	369	369
$1.250 < s < 1.300$	0.1204	0.0917	0.0798	0.949	242	62	62
Nonius CAD-4 Mo $K\alpha$ radiation							
$s < 0.500$	0.0210	0.0342	0.0148	0.876	3620	207	208
$0.500 < s < 0.600$	0.0160	0.0227	0.0173	0.825	741	146	146
$0.600 < s < 0.650$	0.0125	0.0152	0.0151	0.867	541	94	94
$0.650 < s < 0.700$	0.0160	0.0218	0.0184	0.762	434	111	111
$0.700 < s < 0.750$	0.0242	0.0254	0.0255	0.918	510	130	130
$0.750 < s < 0.800$	0.0253	0.0284	0.0275	0.937	606	152	152
$0.800 < s < 0.850$	0.0257	0.0292	0.0268	0.924	650	160	161
$0.850 < s < 0.900$	0.0303	0.0328	0.0295	0.804	782	189	189
$0.900 < s < 0.950$	0.0343	0.0322	0.0344	0.895	836	210	210
$0.950 < s < 1.000$	0.0371	0.0365	0.0352	0.879	918	236	236
$1.000 < s < 1.050$	0.0358	0.0338	0.0348	0.845	1011	255	255
$1.050 < s < 1.100$	0.0423	0.0366	0.0408	0.955	840	282	283
$1.100 < s < 1.150$	0.0412	0.0320	0.0443	1.085	606	303	306
$1.150 < s < 1.200$	0.0448	0.0344	0.0467	1.115	614	307	340
$1.200 < s < 1.250$	0.0424	0.0313	0.0463	1.210	224	112	124

Y interval	R_1	R_2	wR	Z	Number of terms	Number of means
Nonius CAD-4 Ag $K\alpha$ radiation						
$0.0 < Y < 1.0$	0.8781	0.9461	0.6593	0.899	1535	388
$1.0 < Y < 3.0$	0.4448	0.5487	0.2519	0.918	2003	484
$3.0 < Y < 10.0$	0.1266	0.1731	0.0858	0.900	2786	689
$10.0 < Y < 30.0$	0.0442	0.0580	0.0374	0.880	2854	687
$30.0 < Y < 100.0$	0.0242	0.0338	0.0215	0.884	2075	492
$100.0 < Y < 300.0$	0.0158	0.0227	0.0141	0.777	1458	201
$300.0 < Y < 1000.0$	0.0151	0.0225	0.0120	0.671	1917	70
$1000.0 < Y < 3000.0$	0.0257	0.0341	0.0202	1.145	357	10
Nonius CAD-4 Mo $K\alpha$ radiation						
$0.0 < Y < 1.0$	0.8905	0.9455	0.7214	0.995	598	194
$1.0 < Y < 3.0$	0.4206	0.5226	0.2261	0.900	971	281
$3.0 < Y < 10.0$	0.1306	0.1751	0.0953	0.956	1657	471
$10.0 < Y < 30.0$	0.0478	0.0619	0.0414	0.934	2114	561
$30.0 < Y < 100.0$	0.0272	0.0358	0.0239	0.908	2714	661
$100.0 < Y < 300.0$	0.0196	0.0280	0.0166	0.937	2096	387
$300.0 < Y < 1000.0$	0.0155	0.0226	0.0132	0.865	1545	176
$1000.0 < Y < 3000.0$	0.0213	0.0338	0.0139	0.844	835	40
$3000.0 < Y < 10000.0$	0.0275	0.0379	0.0213	1.433	53	4

$\sin\theta/\lambda > 0.85$ $\mathring{A}^{-1}$, the exposure time of $t = 25$ s and a sample-to-detector distance $d = 5$ cm with Ag $K\alpha$ radiation used for the collection of the Nonius Kappa CCD set II data appear to be insufficient to retrieve the maximum number of unique data measurements. Moreover, the agreement factors for the Smart CCD experiment are the best with an equivalent redundancy in Nonius Kappa CCD data set I in the high-resolution

space. On the other hand, the 100 s image-acquisition time permitted measurement of more high-resolution X-ray diffraction intensities up to $(\sin\theta/\lambda)_{max}$ = 1.43 Å^{-1}. We note that in the resolution range 1.05 < $\sin\theta/\lambda$ < 1.10 Å^{-1}, only 222 unique reflections were measured in the Siemens Smart CCD experiment, compared with 287 found in the Nonius Kappa CCD data set I experiment.

Table 2 also gives the merging factors as a function of the squared observed structure factors $|F_o|^2$ on an arbi-

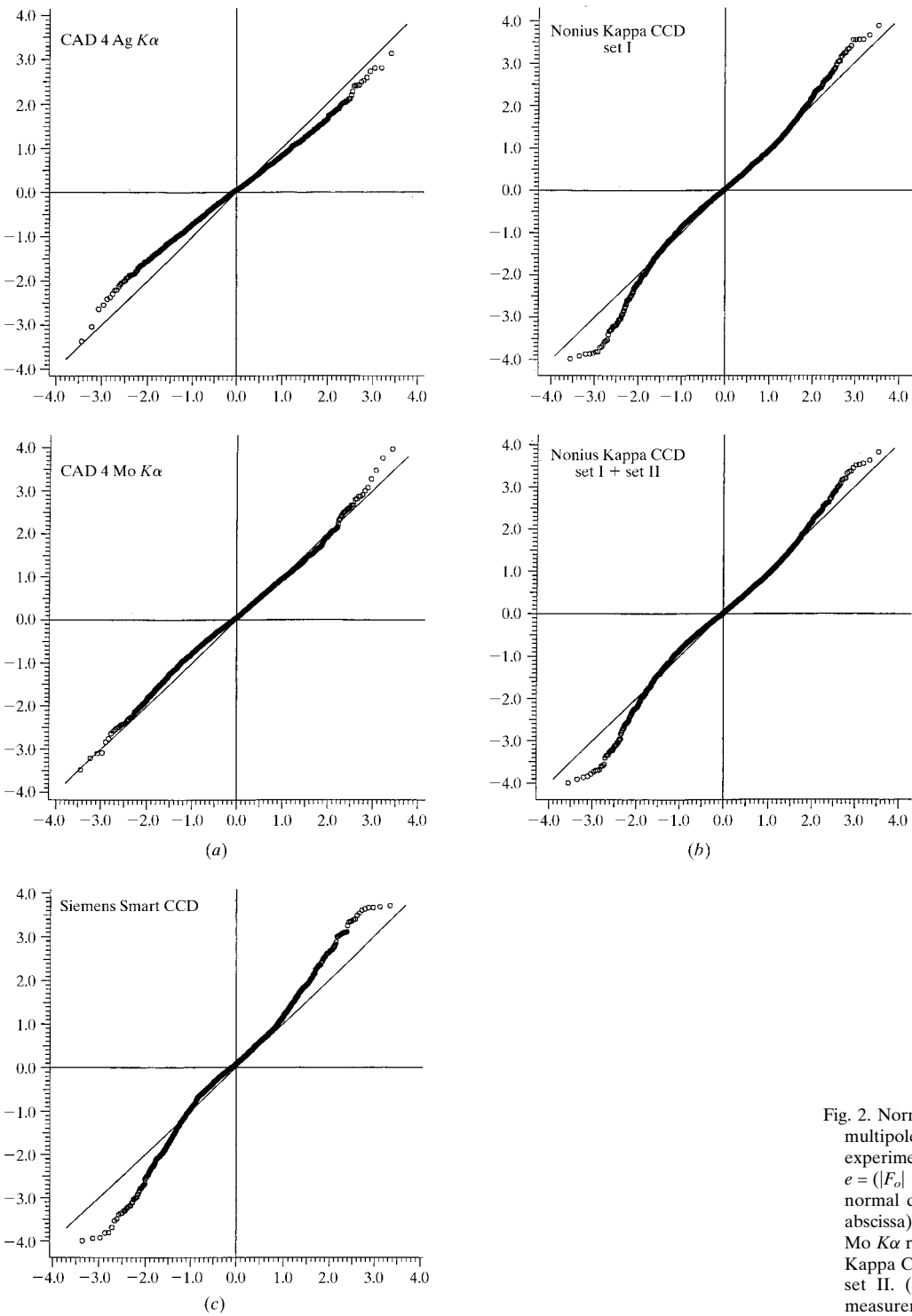

Fig. 2. Normal probability plot after multipole refinements (Table 4); experimental weighted residuals $e = (|F_o| - |F_{calc}|)/\sigma(|F_o|)$ *versus* normal distribution quantiles (on abscissa). (*a*) CAD-4 Ag $K\alpha$ and Mo $K\alpha$ radiation data. (*b*) Nonius Kappa CCD data set I and set I + set II. (*c*) Siemens Smart CCD measurements.

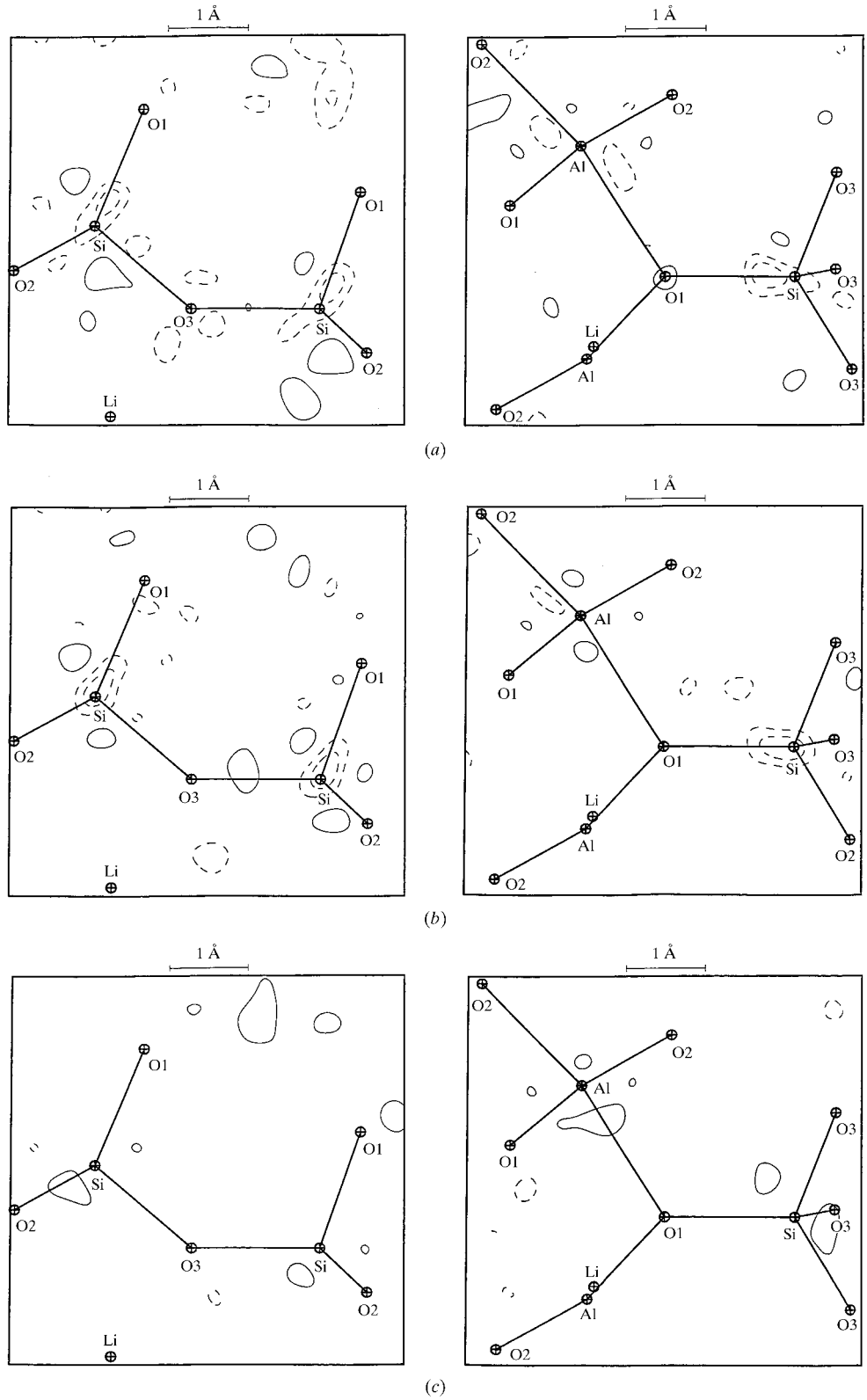

Fig. 3. Residual electron density in Si—O3—Si and Si—O1—Al planes in α-spodumene after the multipole refinements against the CCD data. (*a*) Kappa CCD data set I. (*b*) Kappa CCD data set I + set II. (*c*) Siemens Smart CCD measurements. Contour intervals ± 0.1 e Å^{-3}; negative contours are dashed, the zero contour is omitted. (Fourier summation over data with $0 \leq \sin\theta/\lambda \leq 0.9$ Å^{-1}.)

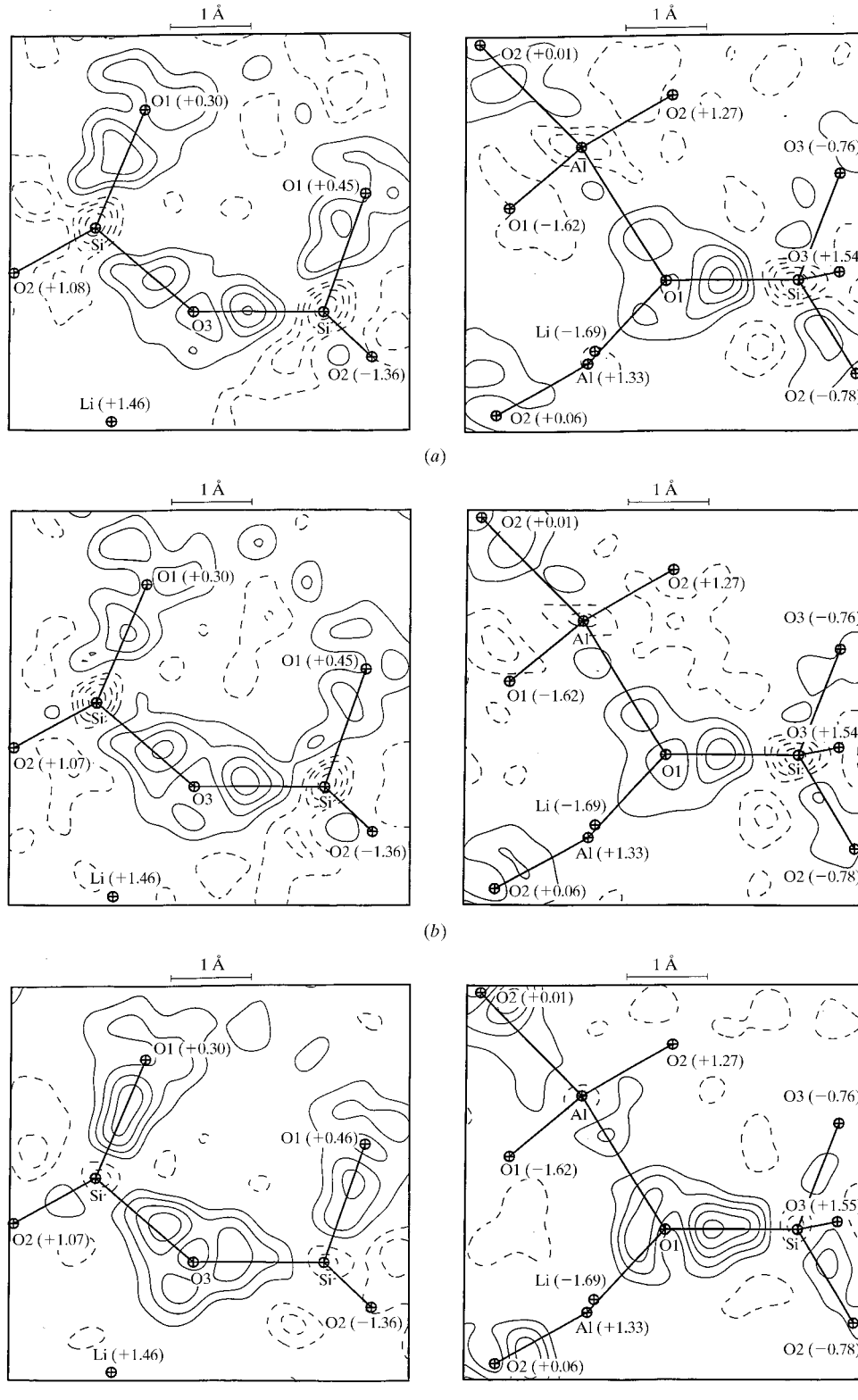

Fig. 4. Experimental electron deformation density in Si—O3—Si and Si—O1—Al planes in α-spodumene after the multipole refinements against the CCD data. (*a*) Kappa CCD data set I. (*b*) Kappa CCD data set I + set II. (*c*) Siemens Smart CCD measurements. Contours as in Fig. 3. The distances to the planes for the out of plane atoms are indicated in parentheses.

Table 4. *Least-squares statistical factors R(F), wR(F) and goodness of fit*

	Kappa CCD set I			Kappa CCD set I + set II			Smart CCD		
Type of refinement	Spherical (IAM)	Multipole	Kappa	Spherical (IAM)	Multipole	Kappa	Spherical (IAM)	Multipole	Kappa
$\sin\theta/\lambda$ (Å^{-1})	1.43	1.43	1.43	1.43	1.43	1.43	1.09	1.09	1.09
Scale factor	2.260 (3)	2.280 (4)	2.284 (1)	2.262 (4) 1.109 (2)†	2.272 (4) 1.113 (2)†	2.277 (2) 1.112 (1)†	0.8184 (14)	0.8126 (10)	0.8153 (4)
$R(F)$ (%)	2.71	2.43	2.60	2.73	2.57	2.67	1.67	1.07	1.39
$wR(F)$ (%)	3.81	3.18	3.48	3.70	2.96	3.24	2.35	1.01	1.54
Goodness of fit	1.28	1.08	1.16	1.32	1.07	1.16	3.19	1.40	2.07
N_{par}	48	138	12	49	139	13	48	138	12
N_{obs} $[I > 3\sigma(I)]$	3692	3692	3692	3680	3680	3680	1743	1743	1743

† Data set II scale factor.

trary scale. Comparing the two Nonius Kappa CCD data sets, the number of terms and the number of averaged reflection intensities are larger for the data set I experiment, realised with t = 100 s and d = 3 cm. However, the consistency factors are lower for data set II, especially for strong reflections (around 4% for set I and 3% for set II). On the other hand, the merging factors of the Siemens Smart CCD data appear to be better (around 3% for medium-to-large diffraction intensity magnitudes) with a superior redundancy in the measurements. However, the Z factors are abnormally high for strong reflection intensities, probably arising from some problem with the experimental error estimates given by the Siemens Smart software.

For comparison, Table 3 gives the agreement factors as a function of resolution and intensity magnitudes for the conventional CAD-4 Ag $K\alpha$ and Mo $K\alpha$ radiation diffraction experiments (Kuntzinger & Ghermani, 1999). The high redundancy of measurements at low resolution is caused by supplementary azimuth Ψ-off reflection scans in order to improve the absorption correction. The very low resolution data have slightly lower statistical averaging indices ($\leq 2\%$) for both the Ag $K\alpha$ and the Mo $K\alpha$ radiation CAD-4 experiment in comparison to the CCD results given in Table 2. However, the agreement factors for $\sin\theta/\lambda$ larger than 0.65 Å^{-1} are quite comparable and even better for all CCD data sets (presumably as a result of the better dynamic performance of the CCD detection), particularly when we take into account the high number of measurements related to each reciprocal resolution shell in these experiments.

3.2. *Statistics of experimental data and error analysis*

The crystallographic refinements are based on a weighted least-squares fit to the experimental data for which uncertainties must in principle be known. The weights are used to put both low-resolution strong intensities or structure factors and high-resolution weak intensities or structure factors on comparable scales in the least-squares procedure. The weights are commonly taken as the inverse of the experimental variances, which are difficult to estimate in an absolute manner. Counting statistics alone are not sufficient to describe the true experimental uncertainties, and systematic errors may be present. For this reason, an 'instability factor', also called the 'ignorance factor', p, was introduced in the case of conventional diffractometer data collections (see McCandlish *et al.*, 1975, and references therein); the variances are then expressed as $\sigma^2(|F_o|^2) = \sigma^2_{\text{counting}}(|F_o|^2) + (p|F_o|^2)^2$, where F_o is the observed structure factor (the intensity $I = |F_o|^2$). This added correction to counting statistics is here related only to the magnitude of the reflection intensity, but other weighting schemes have been tested (see for example Hong & Robertson, 1985, and references therein) to show the influence on the refined crystallographic parameters of constraining the goodness of fit to be close to 1. In order to illustrate for the present study the statistics of our starting data, we have plotted in Fig. 1 the standard uncertainty as a function of the squared structure factor on the experimental arbitrary scale (with $I = |F_o|^2 > 0$). Fig. 1(a) shows the variation of the standard uncertainty for the CAD-4 Ag $K\alpha$ (3022 reflections with $I > 0$) and Mo $K\alpha$ (2818 reflections with $I > 0$) experiments (Kuntzinger & Ghermani, 1999). The CCD data are illustrated in Fig. 1(b) for the Nonius Kappa CCD data sets I (4412 reflections with $I > 0$) and II (1603 reflections with $I > 0$), and in Fig. 1(c) for the Siemens Smart CCD data (2078 reflections with $I > 0$). For the two CAD-4 data sets shown in Fig. 1(a), we note that the standard uncertainties are linear with respect to the squared structure-factor magnitudes. A regression fit (indicated on Fig. 1) of these curves yields slope values of 0.015 for Mo $K\alpha$ and 0.017 for Ag $K\alpha$ radiation, respectively, which are in fact very close to the instrumental instability factors obtained after data processing [p = 0.0130 (2) and 0.0160 (3) for Mo $K\alpha$ and Ag $K\alpha$ radiation, respectively (Kuntzinger & Ghermani, 1999)]. For data corresponding to $I > 3\sigma(I)$ commonly used in refinements, the main contribution to the experimental error comes from the p^2I^2 factor in the estimated variance (McCandlish *et al.*, 1975). The variation of the

Table 5. *Equivalent isotropic displacement parameters U_{eq} ($\times 10^5$ Å^2) obtained after the multipole refinements (Table 4) of the CCD and CAD-4 data*

CAD-4 data according to Kuntzinger & Ghermani (1999).

$$U_{\rm eq} = (1/3)\Sigma_i\Sigma_j U^{ij} a^i a^j \mathbf{a}_i \mathbf{a}_j.$$

	Kappa CCD set I	Kappa CCD set I + set II	Smart CCD	Ag $K\alpha$ CAD-4	Mo $K\alpha$ CAD-4
Si	409 (3)	405 (3)	417 (2)	397 (3)	377 (2)
Al	439 (4)	436 (4)	445 (4)	424 (4)	409 (2)
O1	510 (4)	507 (4)	520 (4)	495 (5)	479 (4)
O2	788 (5)	784 (5)	795 (6)	771 (6)	758 (5)
O3	778 (5)	775 (5)	780 (6)	766 (6)	749 (5)
Li	1506 (35)	1502 (38)	1547 (35)	1474 (40)	1464 (35)

experimental σ in Fig. 1(b) for both Nonius Kappa CCD data sets, I and II, is also linear with respect to $|F_o|^2$. The average slope value is about 0.03 for data set II, which is slightly lower than the value of 0.04 obtained for data set I. We note that the slope values (contrary to the intercept values) are not modified by putting the intensities on an absolute scale. On the other hand, the variation of the standard estimated experimental errors for the Siemens Smart CCD data shown in Fig. 1(c) is not linear with respect to $|F_o|^2$. Furthermore, it is clear that the estimations of the experimental errors of the weak and medium intensities on the one hand and of the strong observations on the other hand are not comparable. The majority of the reflection uncertainties (2033 among 2078 reflections) can be roughly approximated by a linear curve with an average slope value of 0.010, which is very low in comparison to that found for both the Nonius CAD-4 and the Kappa CCD derived errors. The remaining 45 strongest reflections, however, display an overestimation of their standard uncertainties, as shown in Fig. 1(c), and a large dispersion can be noted.

4. Refinements

The least-squares program *MOLLY* (Hansen & Coppens, 1978) was used for both conventional and multipole refinements. The description of the α-spodumene structure, the details of the refinement strategies, the multipole-model definition and parameters are given in our previous paper (Kuntzinger & Ghermani, 1999). In the present study, the refinements were carried out against the Nonius Kappa CCD data set I [3692 reflections up to $(\sin\theta/\lambda)_{\rm max} = 1.43$ Å^{-1} with $I > 3\sigma(I)$] and the Siemens CCD data [1743 reflections up to $(\sin\theta/\lambda)_{\rm max} = 1.09$ Å^{-1} with $I > 3\sigma(I)$], respectively. Other refinements involved a combined Nonius Kappa CCD data set, consisting of data of set I [3347 reflections, $I > 3\sigma(I)$, with $0.6 < \sin\theta/\lambda < 1.43$ Å^{-1}] and a part of set II [333 reflections, $I > 3\sigma(I)$, with $0.0 < \sin\theta/\lambda \leq 0.6$ Å^{-1}], in order to determine the eventual improvement of the low-resolution intensities arising from the supplementary set II data collection.

After the multipole refinements, the atomic net charges in α-spodumene were estimated using the kappa refinement procedure (Coppens *et al.*, 1979). An isotropic secondary-extinction correction corresponding to type I with a Lorentzian mosaic distribution was applied (Becker & Coppens, 1974). The highest intensity correction corresponded to a factor $y = I_{\rm obs}/I_{\rm cor} = 0.70$ for refinement against data set I and was found for the $(\bar{5}31)$ reflection, while $y = 0.65$ for set I + set II (Ag $K\alpha$ X-ray radiation) and $y = 0.44$ for the Smart CCD data set (Mo $K\alpha$ X-ray radiation) were found for the $(\bar{2}21)$ reflection (not present in Nonius data set I). This $(\bar{2}21)$ reflection was corrected by factors $y = 0.68$ and $y = 0.58$ in the CAD-4 Ag $K\alpha$ and Mo $K\alpha$ data refinements (Kuntzinger & Ghermani, 1999) for the same crystal used in the Nonius Kappa CCD experiment. The second, larger sample used for the Siemens CCD data collection exhibited more extinction.

Table 4 gives a summary of the least-squares residual indices after each refinement applied to the CCD detector measurements. It can be noted that the Siemens Smart CCD data refinements have globally lower $R(F)$ and $wR(F)$ factors compared with the Nonius Kappa CCD results. However, even though the number of observations of the Siemens CCD data is smaller, the goodness of fit remains high, probably because of the underestimation of the experimental errors used in the weighted least-squares refinements. On the other hand, a comparison of the Nonius Kappa CCD diffraction data refinements shows that $R(F)$ is slightly better for data set I [$R(F) = 2.43\%$ for multipole refinement for data set I and $R(F) = 2.57\%$ for set I + set II], but $wR(F)$ is larger for data set I [$wR(F) = 3.18\%$ against 2.96% for set I + set II] because of the different weighting schemes related to the estimation of the experimental errors described in §3.2. In order to obtain further insight into the refinement qualities, we have used the method of the normal probability analysis described by Abrahams & Keve (1971) by plotting in Fig. 2 the weighted residuals $e = (|F_o| - |F_{\rm calc}|)/\sigma(|F_o|)$ after the multipole refinements with respect to a normal (Gaussian) distribution. This plot is also called by statisticians the normal quantile plot of residuals, which tests the assumption that the

Table 6. *Atomic kappa parameters and charges in α-spodumene from CCD detector data and comparison with CAD-4 results*

CAD-4 data according to Kuntzinger & Ghermani (1999).

	Kappa CCD set I		Kappa CCD set I + set II		Smart CCD		Ag $K\alpha$ CAD-4		Mo $K\alpha$ CAD-4	
	κ	Charge	κ	Charge	κ	Charge	κ	Charge	κ	Charge
Si	1.11 (2)	1.64 (9)	1.07 (2)	1.55 (8)	1.11 (2)	1.78 (6)	1.18 (2)	1.86 (6)	1.13 (2)	1.73 (6)
Al	1.15 (6)	1.60 (7)	1.11 (5)	1.56 (7)	1.14 (4)	1.42 (6)	1.37 (5)	1.94 (4)	1.10 (4)	1.54 (5)
O1	0.954 (3)	−0.94 (5)	0.956 (3)	−0.85 (5)	0.955 (3)	−0.84 (5)	0.944 (2)	−1.10 (4)	0.950 (2)	−0.95 (4)
O2	0.949 (3)	−0.99 (5)	0.946 (3)	−1.14 (5)	0.945 (3)	−1.03 (5)	0.942 (3)	−1.13 (4)	0.949 (2)	−1.01 (4)
O3	0.948 (3)	−1.02 (6)	0.955 (3)	−0.84 (5)	0.950 (3)	−1.12 (4)	0.949 (3)	−1.10 (4)	0.952 (2)	−1.04 (4)
Li	1.00	1.00	1.00	1.00	1.00	1.00	1.00	1.00	1.00	1.00

errors of the model are normally distributed. In this case, the weighted residuals after the least-squares fit should display a linear curve with an ideal slope value equal to unity and an intercept of zero. The distribution for the CAD-4 experiment (Kuntzinger & Ghermani, 1999) residuals is given in Fig. 2(*a*), which shows excellent linearity for both data sets, with an almost ideal variation for the Mo $K\alpha$ data. The curves corresponding to the Nonius Kappa CCD data set I and set I + set II refinements shown in Fig. 2(*b*) are very similar, but most of the weighted residuals are concentrated in an expected normal distribution range (quantiles) of −2 to +2. On the contrary, for the Siemens Smart CCD refinements (Fig. 2*c*), the linearity is only respected for the central part of the data (in the normal distribution range from −1 to +1), while the remaining majority of the measurements deviates from a normal distribution. This latter feature shows clearly the underestimation of the experimental errors for the Siemens CCD data set and explains the high value of the goodness of fit given in Table 4.

The atomic fractional coordinates, the anisotropic displacement parameters and the Hansen–Coppens model (Hansen & Coppens, 1978) atomic populations after all the multipole refinements are deposited as supplementary material.† With respect to the discrepancies in the unit-cell parameters (Table 1) between CAD-4 and CCD experiments, the bond distances calculated after the multipole refinements against the three CCD data sets are systematically larger (by 10–20 times the standard uncertainties) than those obtained from the conventional diffractometers (see Kuntzinger & Ghermani, 1999), while the bond angles are less affected. The bond distances and angles are also deposited as supplementary material. The equivalent isotropic displacement parameters, U_{eq}, are given in Table 5. For comparison, the last two columns of Table 5 present the results of the CAD-4 data refinements obtained in the previous α-spodumene electron-density study (Kuntzinger & Ghermani, 1999). In Table 5, we note a very good agreement between the CCD U_{eq} parameters; the largest difference appears for the light Li^+ cation. However, in comparison to the CAD-4 results, both the Mo $K\alpha$ and the Ag $K\alpha$ data gave equivalent isotropic displacement parameters that are systematically smaller than those obtained from the CCD data. Fig. 3 displays the residual electron-density maps after the several multipole refinements. The residual electron-density peaks are not significant compared with the experimental errors (Cruickshank, 1949; Rees, 1976): $\langle\sigma^2(\Delta\rho)\rangle^{1/2} = (2/V_{cell})\{\sum_H \sigma^2[K^{-1}|F_o(H)|]\}^{1/2}$ = 0.08 (Nonius Kappa CCD data set I), 0.07 (Nonius Kappa CCD data set I + set II) and 0.06 e Å^{-3} (Siemens Smart CCD data), and $\langle\sigma^2_{res}\rangle^{1/2} = (2/V_{cell})\{\sum_H[K^{-1}|F_o(H)| - |F_{calc}(H)|]^2\}^{1/2}$ = 0.05 (set I), 0.05 (set I + set II) and 0.04 e Å^{-3} (Smart), where V_{cell} is the unit-cell volume and K is the scale factor. All the $\langle\sigma^2(\Delta\rho)\rangle^{1/2}$ values are systematically larger than the $\langle\sigma^2_{res}\rangle^{1/2}$ values obtained after the multipole model fit. This also shows an underestimation of the experimental errors of the CCD data.

5. Results and discussion

5.1. *Experimental deformation electron density*

The electron-density study of the α-spodumene $LiAl(SiO_3)_2$ is a part of our research on the aluminosilicate materials [natrolite $Na_2Al_2Si_3O_{10}.2H_2O$ (Ghermani *et al.*, 1996); scolecite $CaAl_2Si_3O_{10}.3H_2O$ (Kuntzinger *et al.*, 1998)]. The α-spodumene compound belongs to the mineralogical pyroxene group with infinite oxygen-corner silicon-tetrahedra chains along the *c* axis (Clark *et al.*, 1969; Kuntzinger & Ghermani, 1999). The aluminium atom and the Li^+ cation lie in distorted oxygen octahedra between the silicate chains, while the aluminium atoms in the zeolitic natrolite and scolecite crystals are tetrahedrally oxygen coordinated. Therefore, the Si—O and the Al—O bonds in α-spodumene mineral are in a different configuration with respect to natrolite and scolecite.

A first characterization of the electron density of these bonds has been made from high-resolution two-wavelength X-ray diffraction CAD-4 data (Kuntzinger & Ghermani, 1999). In the present study, we have chosen the Si—O—Si bond of the silicate chain (Si—

† Supplementary data for this paper are available from the IUCr electronic archives (Reference: SH0132). Services for accessing these data are described at the back of the journal.

O3—Si) and an Si—O—Al (Si—O1—Al) bridge in order to illustrate the quality of the CCD data and to validate the use of such detectors in the charge-density research. In Fig. 4 we present the experimental deformation density, calculated as

$$\Delta\rho = (1/V_{\rm cell})\Big\{\sum_{H}[K^{-1}|F_o|\exp(i\varphi_{\rm mult}) - |F_{\rm spher}|\exp(i\varphi_{\rm spher})]\exp(-2\pi i\mathbf{H}\cdot\mathbf{r})\Big\},$$

where K is the scale factor, and $|F_o|$ and $|F_{\rm spher}|$ are the observed and calculated spherical structure-factor moduli phased by $\varphi_{\rm mult}$ and $\varphi_{\rm spher}$ after the multipole and the spherical (IAM, independent atomic model) models, respectively. For all the maps shown in Fig. 4, only reflections $[I > 3\sigma(I)]$ with $\sin\theta/\lambda \leq 0.9$ Å^{-1} were included in the Fourier synthesis (1135 reflections for Kappa CCD set I, 1123 for set I + set II, and 1060 for Smart CCD). Very good agreement has been reported (Kuntzinger & Ghermani, 1999) between the experimental deformation electron density and that derived from the multipole model calculations (static). The same holds for the present study. The static maps have been deposited as supplementary material; these maps are also very similar to those from the CAD-4 study (Kuntzinger & Ghermani, 1999). All the maps of Fig. 4 display common features of aluminosilicate compounds (Ghermani *et al.*, 1996; Kuntzinger *et al.*, 1998; Kuntzinger & Ghermani, 1999): a concentration of the electron density around the O atoms and a polarization towards the cations in the structure. On the other hand, the more covalent character of the Si—O bond in comparison to the Al—O link in both tetrahedral (natrolite, scolecite) or octahedral (spodumene) coordination is also revealed in the maps presented in Fig. 4. With respect to the experimental error in electron density given in the previous section, all these maps carry the same information on charge density distribution in α-spodumene; we note, however, that those from the Nonius Kappa CCD joint data set, I + II (Fig. 4*b*), display less bonding electron density than those from data set I (Fig. 4*a*). This shows that the expected improvement of low-resolution reflections in set II is not so evident. The main differences between the experimental electron deformation density maps in Fig. 4 from the Nonius and Siemens data are the more pronounced negative holes on the silicon-atom sites for the Nonius Kappa CCD maps (set I or set I + set II), which were also observed in the previous study (Kuntzinger & Ghermani, 1999). However, these negative holes (shown in Figs. 4*a* and 4*b*) are elongated along the Si—O1 bond, which pushes the electron density towards the oxygen atom in the case of Nonius Kappa CCD data refinements. No explanation of these particular features has been found.

5.2. *Net atomic charges*

The net atomic charges in α-spodumene have been determined using the kappa model refinement (Coppens *et al.*, 1979). As in the previous study, the +1 charge of the Li^+ cation was not refined. Table 6 gives the charges and atomic contraction–expansion kappa parameters (Coppens *et al.*, 1979) from the refinement against the CCD data compared with the CAD-4 data results. In our previous study of electron density and Madelung potential in α-spodumene (Kuntzinger & Ghermani, 1999), we emphasized the correlation between the kappa parameter and the net atomic charge. A discrepancy was reported between the CAD-4 Ag $K\alpha$ and Mo $K\alpha$ results, especially for the Al atom. This yielded a significant difference in the net charge obtained for this atom [κ = 1.37 (5) and q = 1.94 e for Ag $K\alpha$ radiation, and κ = 1.10 (4) and q = 1.54 e for Mo $K\alpha$ radiation], while the differences for Si and O atoms did not exceed 0.15 e (see Table 6). In the present study, as shown in Table 6, a much more stable value for the aluminium kappa parameter was obtained from all the CCD data, with an average value of 1.13, which is close to previous CAD-4 Mo $K\alpha$ radiation results (Kuntzinger & Ghermani, 1999, and references therein). With respect to the standard uncertainties (agreeing to within 3–4 times the standard uncertainties), an excellent agreement and consistency can be noted between all the charges derived from CCD data on the one hand, and the CCD data charges and CAD-4 Mo $K\alpha$ radiation results on the other hand (last column in Table 6). The agreement between the atomic charge values derived from CCD and CAD-4 data is even better than that reported by Martin & Pinkerton (1998) for the organic compound oxalic acid. Consequently, our previous estimation of electrostatic properties, such as the Madelung potential (Kuntzinger & Ghermani, 1999), using conventional CAD-4 data results is entirely recovered by the CCD measurements in the case of α-spodumene. It is worth noting that the four missing low-resolution reflections in the Nonius Kappa CCD data set I (see §3.1) do not notably influence the kappa parameters and the net charge results when compared to those derived from the joint set I + set II refinement.

6. Conclusions

High-resolution X-ray diffraction data sets collected on both Nonius and Siemens CCD detector instruments have been used for a charge-density study of α-spodumene. The obtained good quality CCD data have been compared to those of two X-ray radiation measurements collected on a conventional CAD-4 single-counter diffractometer. However, the main difference appeared in the estimation of the experimental errors between the Nonius and Siemens CCD data. This was revealed by a careful inspection of the statistical factors and the

weighted residuals at the end of the least-squares refinements. In spite of the discrepancy in the least-squares weighting schemes related to the estimated experimental errors, the main electron-density features in the Si—O—Si and Si—O—Al bridges derived from both CCD systems are similar to those determined from the CAD-4 measurements. Furthermore, the net atomic charges and kappa parameters are also in very good agreement. We are, however, convinced that this agreement would be better with an improvement of the estimation of the experimental errors, which is not an easy task given the near 'black box' nature of the Nonius and Siemens CCD processing software. For this purpose and in order to check the influence on the fitted parameters, we have artificially imposed the weighting schemes used for the CAD-4 Ag $K\alpha$ radiation data on the Nonius Kappa CCD set I refinements: the σ distribution slope of 0.017 obtained for the CAD-4 experiment given in §3.2 was used to modify the errors for the CCD data instead of the original value of 0.04. The original CCD diffraction intensities have not been changed; for comparison the variation of the $I_{CCD}/I_{CAD\text{-}4}$ ratios for the common reflections (2251) as a function of $\sin\theta/\lambda$ is given as supplementary material. The modified weighting schemes yield a decrease of the atomic displacements towards those obtained with the CAD-4 data (given in Table 5). This result probably arises from the increase of the weights of the high-resolution data in the least-squares procedure. Furthermore, additional bond electron-density peaks of ~ 0.1 e Å^{-3} appear on the experimental electron deformation density maps. Weight modification was not tried with the Siemens CCD data because of the noted discrepancy in the respective variations of the standard uncertainties of the intense reflections and those of the medium and weak intensities. In conclusion, the CCD data are quite suitable for charge-density studies, even for mineral materials. However, the difficult problem of the experimental error estimates should be solved for such new systems in order to bring the CCD and the CAD-4 measurements to the same level of quality.

We would like to thank Drs M. Adam and B. Schierbeek and the staff of the Nonius company in Delft (The Netherlands) for their helpful collaboration in collecting the α-spodumene Kappa CCD data sets. The financial support of the CNRS, the Université Henri Poincaré, Nancy 1 (France), and the University of Durham (UK) is gratefully acknowledged.

References

Abrahams, S. C. & Keve, E. (1971). *Acta Cryst.* A**27**, 157–165.
Allinson, N. M. (1994). *J. Synchrotron Rad.* **1**, 54–62.
Becker, P. J. & Coppens, P. (1974). *Acta Cryst.* A**30**, 129–147.
Blessing, R. H. (1987). *Crystallogr. Rev.* **1**, 3–58.
Blessing, R. H. (1989). *J. Appl. Cryst.* **22**, 396–397.
Blessing, R. H. (1995). *Acta Cryst.* A**51**, 33–38.
Bolotovsky, R., Darovsky, R., Kezerashvili, V. & Coppens, P. (1995). *J. Synchrotron Rad.* **2**, 181–184.
Clark, J. R., Appleman, D. E. & Papike, J. J. (1969). *Mineral. Soc. Am. Spec. Pap.* **2**, 31–50.
Coppens, P., Carducci, M., Bolotovsky, R. & Zaleski, J. (1997). *Proceedings of Sagamore XII. Charge, Spin and Momentum Densities*, 27 July to 1 August 1997, Waskesiu, Canada. Abstract RA52.
Coppens, P., Guru, T. N., Leung, P., Stevens, E. D., Becker, P. & Yang, Y. W. (1979). *Acta Cryst.* A**35**, 63–72.
Cruickshank, D. W. J. (1949). *Acta Cryst.* **2**, 65–82.
Dahaoui, S., Jelsch, C., Howard, J. A. K. & Lecomte, C. (1999). *Acta Cryst.* B**55**, 226–230.
Diamond, R. (1969). *Acta Cryst.* A**25**, 43–55.
Ghermani, N. E., Lecomte, C. & Dusausoy, Y. (1996). *Phys. Rev. B*, **53**, 5231–5239.
Graafsma, H., Souhassou, M., Puig-Molina, A., Harkema, S., Kvick, Å & Lecomte, C. (1997). *Proceedings of Sagamore XII. Charge, Spin and Momentum Densities*, 27 July to 1 August 1997, Waskesiu, Canada. Abstract RA53.
Graafsma, H., Souhassou, M., Puig-Molina, A., Harkema, S., Kvick, Å. & Lecomte, C. (1998). *Acta Cryst.* B**54**, 193–195.
Graafsma, H., Svensson, S. O. & Kvick, Å. (1997). *J. Appl. Cryst.* **30**, 957–962.
Hansen, N. K. & Coppens, P. (1978). *Acta Cryst.* A**34**, 909–921.
Hong, W. & Robertson, B. E. (1985). *Structure and Statistics in Crystallography. Proceedings of the Symposium on Crystallographic Statistics*, edited by A. J. C. Wilson. Guilderland, New York: Adenine Press.
Kirschbaum, K., Martin, A. & Pinkerton, A. A. (1997). *J. Appl. Cryst.* **30**, 514–516.
Koritsanszky, T., Flaig, R., Zobel, D., Krane, H. G., Morgenroth, W. & Luger, P. (1998). *Science*, **279**, 356–358.
Kuntzinger, S. & Ghermani, N. E. (1999). *Acta Cryst.* B**55**, 273–284.
Kuntzinger, S., Ghermani, N. E., Lecomte, C. & Dusausoy, Y. (1998). *Acta Cryst.* B**54**, 819–833.
Macchi, P., Proserpio, D. M. & Sironi, A. (1998). *J. Am. Chem. Soc.* **120**, 1447–1455.
Macchi, P., Proserpio, D. M., Sironi, A., Soave, R. & Destro, R. (1998). *J. Appl. Cryst.* **31**, 583–588.
Martin, A. & Pinkerton, A. A. (1998). *Acta Cryst.* B**54**, 471–477.
McCandlish, E., Stout, G. H., Andrews, L. C. (1975). *Acta Cryst.* A**31**, 245–249.
Nonius (1998). *COLLECT, DENZO, SCALEPACK, SORTAV. Kappa CCD Program Package.* Nonius BV, Delft, The Netherlands.
Pichon-Pesme, V., Lecomte, C., Wiest, R. & Bénard, M. (1994). *J. Am. Chem. Soc.* **98**, 1351–1362.
Pinkerton, A. A. (1997). *Proceedings of Sagamore XII. Charge, Spin and Momentum Densities*. 27 July to 1 August 1997, Waskesiu, Canada. Abstract RM50.
Rees, B. (1976). *Acta Cryst.* A**32**, 483–488.
Sheldrick, G. M. (1996). *SADABS. Siemens Area Detector Absorption Software.* University of Göttingen, Germany.
Siemens (1996). *ASTRO, SAINT and SADABS. Data Collection and Processing Software for the SMART System.* Siemens Analytical X-ray Instruments Inc., Madison, Wisconsin, USA.